



HAL
open science

Growth form defines physiological photoprotective capacity in intertidal benthic diatoms

Alexandre Barnett, Vona Méléder, Lander Blommaert, Bernard Lepetit, Wim Vyverman, Koen Sabbe, Christine Dupuy, Johann Lavaud

► **To cite this version:**

Alexandre Barnett, Vona Méléder, Lander Blommaert, Bernard Lepetit, Wim Vyverman, et al.. Growth form defines physiological photoprotective capacity in intertidal benthic diatoms. The International Society of Microbiological Ecology Journal, 2015, 9, pp.32-45. 10.1038/ismej.2014.105 . hal-01110925

HAL Id: hal-01110925

<https://hal.science/hal-01110925>

Submitted on 29 Jan 2015

HAL is a multi-disciplinary open access archive for the deposit and dissemination of scientific research documents, whether they are published or not. The documents may come from teaching and research institutions in France or abroad, or from public or private research centers.

L'archive ouverte pluridisciplinaire **HAL**, est destinée au dépôt et à la diffusion de documents scientifiques de niveau recherche, publiés ou non, émanant des établissements d'enseignement et de recherche français ou étrangers, des laboratoires publics ou privés.

1 Growth form defines physiological photoprotective capacity in intertidal benthic diatoms

2

3 Alexandre Barnett¹, Vona Méléder^{1,2}, Lander Blommaert^{1,3}, Bernard Lepetit^{1#}, Pierre

4 Gaudin^{1,2§}, Wim Vyverman³, Koen Sabbe³, Christine Dupuy¹ & Johann Lavaud^{1*}

5

6 ¹ UMR7266 LIENSs ‘Littoral, Environnement et Sociétés’, CNRS/Université de La Rochelle,

7 Institut du Littoral et de l’Environnement, 2 rue Olympe de Gouges, 17000 La Rochelle,

8 France.

9 ² UPRES EA 2160 MMS ‘Mer, Molécules, Santé’, Université de Nantes, Faculté des Sciences

10 et Techniques, 2 rue de la Houssinière, BP 92208, 44322 Nantes cedex 3, France.

11 ³ Laboratory of Protistology & Aquatic Ecology, Department of Biology, Ghent University,

12 Krijgslaan 281-S8, B-9000 Ghent, Belgium.

13 * Corresponding author:

14 UMR 7266 ‘LIENSs’, CNRS/Université de La Rochelle, Institut du Littoral et de

15 l’Environnement (ILE), 2 rue Olympe de Gouges, 17000 La Rochelle, France

16 Phone: +33-(0)5-46-50-76-45, Fax: +33-(0)5-46-45-82-64, E-mail: johann.lavaud@univ-lr.fr

17 # Current address: Group of Plant Ecophysiology, Department of Biology, University of

18 Konstanz, Universitätsstraße 10, 78457 Konstanz, Germany

19 § Current address: UMR6112 ‘LPGN’, CNRS / Université de Nantes, Faculté des Sciences et

20 Techniques, 2 rue de la Houssinière, BP 92208, 44322 Nantes cedex 3, France.

21

22 Running title: Photoprotection in intertidal benthic diatoms

23 Keywords: benthic / diatom / intertidal flat / non-photochemical quenching / photoprotection /

24 xanthophyll

25 Subject category: Microbial ecology and functional diversity of natural habitats

26 **Abstract**

27 In intertidal marine sediments, characterized by rapidly fluctuating and often extreme light
28 conditions, primary production is frequently dominated by diatoms. We performed a
29 comparative analysis of photophysiological traits in 15 marine benthic diatom species
30 belonging to the four major morphological growth forms (epipelon, motile and non-motile
31 epipsammon and tychoplankton) found in these sediments. Our analyses revealed a clear
32 relationship between growth form and photoprotective capacity, and identified fast regulatory
33 physiological photoprotective traits (i.e. non-photochemical quenching and the xanthophyll
34 cycle) as key traits defining the functional light response of these diatoms. Non-motile
35 epipsammon and motile epipelon showed the highest and lowest non-photochemical
36 quenching respectively, with motile epipsammon showing intermediate values. Like epipelon,
37 tychoplankton had low non-photochemical quenching, irrespective of whether they were
38 grown in benthic or planktonic conditions, reflecting an adaptation to a low light
39 environment. Our results thus provide the first experimental evidence for the existence of a
40 trade-off between behavioural (motility) and physiological photoprotective mechanisms (non-
41 photochemical quenching and the xanthophyll cycle) in the four major intertidal benthic
42 diatoms growth forms using unialgal cultures. Remarkably, while motility is restricted to the
43 raphid pennate diatom clade, raphid pennate species which have adopted a non-motile
44 epipsammic or a tychoplanktonic life style display the physiological photoprotective response
45 typical of these growth forms. This observation underscores the importance of growth form
46 and not phylogenetic relatedness as the prime determinant shaping the physiological
47 photoprotective capacity of benthic diatoms.

48

49 **Introduction**

50 Functional trait-based approaches are increasingly adopted to explain and understand the
51 distribution and diversity of phytoplankton communities (Litchman and Klausmeier, 2008;
52 Barton *et al.*, 2013; Edwards *et al.*, 2013). Various morphological and physiological traits
53 have been shown to define the ecological niches of phytoplankton species, including size,
54 temperature response and resource acquisition and utilization traits. For example, in
55 planktonic diatoms, which play a key role in marine primary production and biogeochemical
56 cycling (Armbrust, 2009), pronounced species-specific differences in photosynthetic
57 architecture and photophysiological strategies have been documented (e.g. Dimier *et al.*,
58 2007; Key *et al.*, 2010; Schwaderer *et al.*, 2011; Wu *et al.*, 2012) and related to their *in situ*
59 light environment (Strzepek and Harrison, 2004; Lavaud *et al.*, 2007; Dimier *et al.*, 2009;
60 Petrou *et al.*, 2011). A high capacity for physiological photoprotection is generally observed
61 in highly fluctuating light climates and/or under on average high irradiances. This suggests
62 that photoprotective capacity is an adaptive trait that shapes the distribution of planktonic
63 diatoms in the environment (Lavaud *et al.*, 2007; Dimier *et al.*, 2009; Bailleul *et al.*, 2010;
64 Petrou *et al.*, 2011; Lavaud and Lepetit, 2013).

65 Benthic marine environments, and especially intertidal environments, are characterized by
66 even more changeable and extreme light climates resulting from the interplay of weather
67 conditions, tides, water column turbidity and sediment composition (and hence light
68 penetration) (Admiraal, 1984; Underwood and Kromkamp, 1999; Paterson and Hagerthey,
69 2001). Nevertheless, intertidal sediments rank amongst the most productive ecosystems on
70 Earth, largely owing to the primary production of highly diverse assemblages of benthic
71 diatoms (Underwood and Kromkamp, 1999). To date however, little is known about the role
72 of functional traits, and especially photophysiological traits, in shaping the structure,

73 dynamics and function of benthic diatom assemblages. In most studies, diatom functional
74 groups are defined on the basis of morphological growth form (e.g. Gottschalk and Kahlert,
75 2012; Larson and Passy, 2012) and not physiological traits. In addition, photoprotective
76 ability (limited to the measurement of the ‘xanthophyll cycle’, XC) and its relationship with
77 ecology has only been studied in natural communities with mixed assemblages of functional
78 groups (e.g. Jesus *et al.*, 2009; van Leeuwe *et al.*, 2009; Cartaxana *et al.*, 2011).

79 In temperate seas, intertidal benthic communities are largely dominated by diatoms (Méléder
80 *et al.*, 2007; Ribeiro *et al.*, 2013), which display a high degree of taxonomic, phylogenetic and
81 functional diversity (Kooistra *et al.*, 2007). Several growth forms can be distinguished, which
82 mainly differ in their attachment mode and degree of motility (see Ribeiro *et al.* (2013) for a
83 detailed description): (1) the epipelon (EPL) comprises larger (usually > 10 µm) motile
84 diatoms which can move freely in between sediment particles and typically form biofilms (cf.
85 (Herlory *et al.*, 2004); (2) the epipsammon (EPM) groups smaller (usually < 10 µm) diatoms
86 which live in close association with individual sand grains; and (3) the tychoplankton
87 (TYCHO), which is an ill-defined and rather enigmatic group of largely non-motile diatoms
88 which presumably have an amphibious life style (both sediment and water column) (e.g.
89 Sabbe *et al.* (2010)). Within the epipsammic group, non-motile (EPM-NM) species are firmly
90 attached (either stalked or adnate) to sand particles, while motile forms (EPM-M) can move
91 within the sphere of individual sand grains. From a phylogenetic perspective, motile forms
92 (i.e. all epipelon and motile epipsammon) exclusively belong to the pennate raphid clade
93 (Kooistra *et al.*, 2007), possessing a raphe allowing motility. Most non-motile epipsammon
94 belongs to the pennate araphid lineage, but also includes some raphid pennates, such as
95 *Biremis lucens*, which firmly attaches to sand grains (Sabbe *et al.*, 1995). Tychoplankton
96 includes both centric and pennate raphid forms. Intertidal benthic diatom species, but also

97 growth forms, show distinct distribution patterns in time and space, suggesting pronounced
98 (micro)niche differentiation (Sabbe, 1993; Méléder *et al.*, 2007, Ribeiro *et al.*, 2013). For
99 example, epipsammon dominates non-cohesive sandy sediments (Méléder *et al.*, 2007), while
100 epipelon dominates cohesive muddy sediments (Haubois *et al.*, 2005). Epipelon typically
101 display vertical ‘micromigration’ in the sediment following endogenous tidal/dial rhythms
102 and environmental stimuli (Saburova and Polikarpov, 2003; Consalvey *et al.*, 2004; Coelho *et*
103 *al.*, 2011): during daylight emersion, they migrate to the sediment surface, while during
104 immersion they migrate to deeper sediment layers.

105 To prevent photoinhibition (Serôdio *et al.*, 2008), benthic diatoms utilize behavioural and
106 physiological responses (Mouget *et al.*, 2008; van Leeuwe *et al.*, 2009; Perkins *et al.*, 2010b;
107 Cartaxana *et al.*, 2011; Serôdio *et al.*, 2012). Behavioural photoprotection involves motility,
108 allowing cells to position themselves in light gradients and escape from prolonged exposure
109 to excess light (Admiraal, 1984; Kromkamp *et al.*, 1998; Consalvey *et al.*, 2004; Serôdio *et*
110 *al.*, 2006). In addition, both motile and non-motile species employ fast regulatory
111 physiological processes for photoprotection (i.e. ‘physiological photoprotection’; Lavaud,
112 2007; Goss and Jakob, 2010; Depauw *et al.*, 2012; Lepetit *et al.*, 2012). In diatoms, two
113 processes are important in field situations (Lavaud, 2007): photosystem II cyclic electron
114 transfer (PSII CET) and non-photochemical quenching of chlorophyll (Chl) fluorescence
115 (NPQ) (Depauw *et al.*, 2012; Lepetit *et al.*, 2012; Lavaud and Lepetit, 2013). NPQ is
116 controlled by several regulatory partners including the light-dependent conversion of
117 diadinoxanthin (DD) to diatoxanthin (DT) by the DD de-epoxidase (i.e. the XC) (Brunet and
118 Lavaud, 2010; Goss and Jakob, 2010). In benthic diatoms however, XC-NPQ has only rarely
119 been studied, and mostly *in situ*: it has been shown to vary with diurnal and tidal cycles,
120 season, latitude (Serôdio *et al.*, 2005; van Leeuwe *et al.*, 2009; Chevalier *et al.*, 2010), the

121 organisms' position within the sediments and along the intertidal elevation gradient (Jesus *et*
122 *al.*, 2009; Cartaxana *et al.*, 2011). On the basis of their *in situ* measurements, the latter authors
123 hypothesized the existence of a trade-off between behavioural and physiological
124 photoprotection mechanisms in benthic diatoms as a stronger XC was shown to occur in
125 sandy *vs.* muddy sediments. However, at least the sandy sediments contained a mix of both
126 epipsammic and epipellic forms (Jesus *et al.*, 2009; Cartaxana *et al.*, 2011), and even when the
127 latter are not numerically dominant, they can still make a substantial contribution to biomass
128 due to their much larger biovolumes (see e.g. Hamels *et al.* 1998).

129 Our study represents a comprehensive characterization of fast regulatory physiological
130 photoprotection capacity in typical representatives of the major diatom growth forms
131 occurring in intertidal marine sediments. Given the highly dynamic and often extreme
132 intertidal light climate, we hypothesize that photoprotective features are key traits shaping
133 niche differentiation between benthic growth forms, as has been proposed before for
134 phytoplankton (Huisman *et al.*, 2001; Litchman and Klausmeier, 2008; Dimier *et al.*, 2009;
135 Petrou *et al.*, 2011; Lavaud and Lepetit, 2013). In this respect, we predict that the largely
136 immotile epipsammic life forms are better able to cope with pronounced and rapid changes in
137 light intensity at the physiological level than the motile epipellic forms which can actively
138 position themselves in the sediment light gradient.

139

140 **Materials and methods**

141 *Diatom culturing and harvesting (Table 1)*

142 Fifteen benthic diatom strains were used (Table 1). All species were assigned to their
143 respective growth form on the basis of microscopical observations on natural assemblages.
144 They were grown in batch cultures at 20°C in sterile artificial F/2 seawater medium enriched
145 with NaHCO₃ (80 mg L⁻¹ final concentration). Tychoplankton species were also grown in
146 continuously flushed airlift (i.e. with air bubbling) to mimic ‘planktonic’ growth conditions.
147 Two light intensities (E, 20 and 75 μmol photons m⁻² s⁻¹) were used with a 16 h light:8 h dark
148 photoperiod white fluorescent tubes, L58W/840, OSRAM, Germany. Cultures were
149 photoacclimated to the above conditions at least 2 weeks before measurements and
150 experiments (see below). Diatom suspensions for the experiments were prepared to a final
151 concentration of 10 μg chlorophyll *a* (Chl *a*) mL⁻¹. For this purpose, Chl *a* concentration was
152 determined according to the (Jeffrey and Humphrey, 1975) spectrophotometric method.
153 Diatoms suspensions were continuously stirred at 20°C under the growth E (i.e. 20 or 75
154 μmol photons m⁻² s⁻¹) at least 1 h before the start of the experiments and all along the course
155 of the experiments (Lavaud *et al.*, 2007). This kept the photosynthetic machinery in an
156 oxidized state and prevented NPQ.

157

158 *Growth rates and biovolumes*

159 Specific growth rates, μ (d⁻¹), were calculated from regression of the natural logarithm of the
160 number of diatom cells during their exponential growth phase as microscopically determined
161 in a Malassez’s counting chamber. Biovolumes (μm³) were calculated using the formula of
162 (Hillebrand *et al.*, 1999) based on measurements performed on fifteen specimens per species.

163

164

165 *HPLC pigment analyses*

166 Chl *a*, Chlorophyll *c* (Chl *c*), fucoxanthin (Fx), DD, DT and β -carotene (β -car) content, all
167 normalized to Chl *a* (i.e. expressed as mol. 100 mol Chl *a*⁻¹), were measured using HPLC as
168 described in Jakob *et al.* (1999). 1 mL of diatom suspension was rapidly filtered (Isopore 1.2
169 μ m RTTP filters, Merck Millipore, Ireland) and immediately frozen in liquid nitrogen before
170 extraction in a cold (4°C) mixture of 90% methanol/0.2 M ammonium acetate (90/10 vol/vol)
171 and 10% ethyl acetate. The pigment extraction was improved by the use of glass beads
172 (diameter 0.25-0.5 mm, Roth, Germany) and included several short (20 s) vortexing steps.
173 Supernatants were collected after centrifugation (5 min, 10 000 g, 4°C) and immediately
174 injected into an HPLC system (Hitachi Lachrom Elite, Japan) equipped with a cooled auto-
175 sampler and a photodiode array detector (L-2455). Chromatographic separation was carried
176 out using a Nucleosil 120-5 C18 column (125 mm long, 4 mm internal diameter, 5 μ m
177 particles, Macherey-Nagel, Germany) equipped with a pre-column (CC 8/4 Nucleosil,
178 Macherey-Nagel, Germany) for reverse phase chromatography during a 25 min elution
179 program. The solvent gradient followed Jakob *et al.* (1999) with an injection volume of 50 μ L
180 and a flow rate of 1.5 mL min⁻¹. Pigments were identified from absorbance spectra (400-800
181 nm) and retention times (Roy *et al.*, 2011), and their concentrations were obtained from the
182 signals in the photodiode array detector at 440 nm. The de-epoxidation state (DES in %) was
183 calculated as [(DT / DD + DT) x 100], where DD is the epoxidized form and DT is the de-
184 epoxidized form. Chl *a* concentration per cell was determined during exponential growth
185 based on cell counts (see above) and the Chl *a* measurements.

186

187 *Chl fluorescence yield and light curves (Table 2)*

188 For a complete overview of the definition and measurement of the photophysiological
189 parameters, see Table 2. Chl fluorescence yield was monitored with a Diving-PAM

190 fluorometer (Walz, Germany) on a 2.5 mL stirred and 20°C controlled diatom suspension
191 (Lavaud et al 2004). Before measurement, the cells were dark-adapted for 15 min, and a
192 saturating pulse ($3600 \mu\text{mol photons m}^{-2} \text{s}^{-1}$, duration 0.4 ms) was fired to measure F_0 , F_m and
193 F_v/F_m . Two types of light curves were performed: Non Sequential and Rapid Light Curves
194 (NSLCs and RLCs) (Perkins *et al.*, 2010a). For NSLCs, continuous light (KL-2500 lamp,
195 Schott, Germany) was applied for 5 min at different E_s ($48\text{-}1950 \mu\text{mol photons.m}^{-2}.\text{s}^{-1}$); a new
196 diatom suspension was used for each E . At the end of each exposure, F_m' and NPQ were
197 measured. For RLCs, one diatom suspension was exposed to 8 successive, incrementally
198 increasing E_s ($29\text{-}1042 \mu\text{mol photons.m}^{-2}.\text{s}^{-1}$) of 30 s each (Perkins *et al.*, 2006) (Table S1).
199 RLCs allow constructing rETR *vs.* E and NPQ *vs.* E curves. The NPQ *vs.* E curve is based on
200 a 3-parameter Hill equation model and it is described by the equation $\text{NPQ}(E) = \text{NPQ}_m \times$
201 $[E^{n_{\text{NPQ}}}/(E_{50_{\text{NPQ}}}^{n_{\text{NPQ}}} + E^{n_{\text{NPQ}}})]$ (Serôdio and Lavaud, 2011). From the fitted rETR- E curves
202 (Eilers and Peeters, 1988) and NPQ- E curves (Serôdio and Lavaud, 2011), $r\text{ETR}_m$, α , E_k , and
203 NPQ_m , $E_{50_{\text{NPQ}}}$, n_{NPQ} can be derived, respectively. All parameters are described in the Table 2.
204 n_{NPQ} is the Hill coefficient or the sigmoidicity coefficient of the NPQ- E curve (Serôdio and
205 Lavaud, 2011). It informs on the onset of NPQ at moderate E_s , i.e. when the DT molecules
206 are being 'activated' with increasing E_s to effectively participate to NPQ: DT 'activation'
207 depends on its enzymatic conversion and its binding to the PSII light-harvesting antenna
208 complex in order to promote the antenna switch to a dissipative state of excess energy which
209 is measurable by NPQ (see Lavaud and Lepetit, 2013). When n_{NPQ} is < 1 , the NPQ- E curve
210 shows an asymptotic saturation-like increase towards NPQ_m , while when n_{NPQ} is > 1 , the
211 NPQ- E curve shows a sigmoidal shape. In the later case, the Hill reaction (i.e. NPQ onset) is
212 allosteric (as proposed for the NPQ mechanism, see Lavaud and Lepetit, 2013), n_{NPQ} thus
213 informing on the degree of allostery of the NPQ- E curve. The higher n_{NPQ} , the more
214 positively cooperative the Hill reaction is; n_{NPQ} around 2 being the highest values reported so

215 far (Serôdio and Lavaud, 2011). The same fitting procedure can obviously be used for the
216 DT-E and the DES-E curves, thereby extracting analogous parameters as from the fitted NPQ-
217 E curves.

218

219 *O₂ yield and the PSII CET*

220 The relative O₂ yield produced during a sequence of single-turnover saturating flashes at a
221 frequency of 2 Hz was measured with a home-made rate electrode (Lavaud *et al.*, 2002). The
222 steady-state O₂ yield per flash (Y_{SS}) was attained for the last 4 flashes of a sequence of 20
223 when the S-state cycle oscillations were fully damped (Lavaud *et al.*, 2002). Y_{SS} of 15 min
224 dark-adapted (**D**) and illuminated (**L**, samples taken at the end of each NSLC) cells was used to
225 calculate the PSII CET (Lavaud *et al.*, 2002; Lavaud *et al.*, 2007) as follows: $[\{(20 \times Y_{SS} \text{ L}) - (\sum (Y_{1...20}) \text{ L})\} - \{(20 \times Y_{SS} \text{ D}) - (\sum (Y_{1...20}) \text{ D})\}] / Y_{SS} \text{ D}$.

227

228 *Statistics*

229 Statistical analyses were conducted using the statistical software package SAS 9.3. Species
230 were compared using the general linear model PROC GLM. Growth forms (groups) were
231 compared using the mixed linear model PROC MIXED. Groups were regarded as fixed
232 effects. Data were log- or square root-transformed when needed to allow the best possible fit.
233 Where necessary, estimated least squares means (lsmeans) and standard errors (SE) were
234 back-transformed as in Jørgensen and Pedersen (1998).

235

236 **Results**

237 *Growth rate and photosynthetic properties (Fig. S1, Tables 3, S2, S3)*

238 The Chl *a* concentration per cell showed an exponential relationship with biovolume with
239 relatively small changes at the smaller cell volumes (Fig. S1) The average diatom
240 biovolumes were independent of growth form (Table 3, Fig. S1). Growth rate did not differ
241 significantly between the growth forms at growth $E = 20 \mu\text{mol photons m}^{-2} \text{ s}^{-1}$. Relative
242 concentrations of the light-harvesting pigments Chl *c* and Fx were comparable among growth
243 forms. β -car, which is mainly associated with the photosystem cores, was only slightly but
244 significantly higher in epipelon than in non-motile epipsammon. DD+DT content was
245 significantly lower in epipelon than in the other growth forms. Because the cells were grown
246 at low *E*, DES was generally low, with no significant differences between the growth forms.
247 The highest DD+DT ($16.95 \pm 2.56 \text{ mol } 100 \text{ mol Chl } a^{-1}$) and DES ($16.4 \pm 6.2 \%$) values were
248 observed in *Plagiogramma staurophorum* (non-motile epipsammon). There were no
249 significant differences in F_v/F_m , α , $rETR_m$, E_k and PSII CET_{max} between the growth forms. E_k
250 was on average 3 to 4 times the growth *E* in all growth forms. PSII CET_m was close to 3 (its
251 maximum, Lavaud *et al.*, 2002) for the two epipsammon growth forms, and about 2 in
252 epipelon and tycho plankton.

253

254 *NPQ properties (Figs 1, S2, Tables 4, S4-S6)*

255 At *E* values $\geq 230 \mu\text{mol photons m}^{-2} \text{ s}^{-1}$, NPQ was significantly higher in non-motile
256 epipsammon than in both epipelon and tycho plankton; the same holds true for motile
257 epipsammon vs. epipelon and tycho plankton at *E* values $\geq 1050 \mu\text{mol photons m}^{-2} \text{ s}^{-1}$. NPQ
258 was also significantly higher in non-motile epipsammon than in motile epipsammon except at
259 the lowest and highest *E* values. Likewise, NPQ_m was significantly higher (x 3.5 and x 2.4,
260 respectively) in non-motile epipsammon and motile epipsammon than in epipelon and

261 tychoplankton. In epipelon and tychoplankton, the NPQ-E curves showed a lower variability
262 than in the two epipsammon growth forms. Non-motile epipsammon had the lowest $E50_{NPQ}$,
263 significantly lower than all other groups. In contrast, tychoplankton $E50_{NPQ}$ was significantly
264 higher than in the other groups. Epipellic and motile epipsammonic $E50_{NPQ}$ did not differ
265 significantly from each other. In contrast, n_{NPQ} was not significantly different and varied
266 around its optimum (i.e. 2, Serôdio and Lavaud, 2011) in most species except the
267 tychoplanktonic ones (which is significantly lower than in epipsammon non-motile).

268

269 *XC properties (Figs 1-2, Tables 4, S4, S6, S7)*

270 DES was only significantly different between epipelon and both tychoplankton and motile
271 epipsammon at $105 \mu\text{mol photons}\cdot\text{m}^{-2}\cdot\text{s}^{-1}$ and between epipelon and both epipsammonic forms at
272 $230 \mu\text{mol photons}\cdot\text{m}^{-2}\cdot\text{s}^{-1}$. DES_m varied between 21.2 ± 3.4 for epipelon, 22.7 ± 4.4 for
273 tychoplankton, 28.7 ± 4.4 for motile epipsammon-M and 29.4 ± 3.8 for non-motile
274 epipsammon (lsmmeans \pm SE). The slight difference between epipelon and the epipsammon
275 growth forms, although not significant, in combination with the significantly higher DD+DT
276 in the latter, generated a significantly lower DT_m in epipelon than in the epipsammon growth
277 forms. $E50_{DT}$ was close to the $E50_{NPQ}$ in all growth forms except in tychoplankton where it
278 was lower; no significant differences between the epipsammon and epipelon were observed,
279 only non-motile epipsammon and tychoplankton $E50_{DT}$ differed significantly. n_{DT} was
280 significantly lower in motile epipsammon and tychoplankton than in epipelon and non-motile
281 epipsammon. NPQ/DT was about half its optimum (= 1 under these experimental conditions)
282 in all groups except non-motile epipsammon. It roughly followed the same order as observed
283 for NPQ_m , i.e. non-motile epipsammon > motile epipsammon > epipelon \cong tychoplankton,
284 with a 2x higher value in non-motile epipsammon. The difference between non-motile
285 epipsammon and the other growth forms, however, was not significant due to the low

286 NPQ/DT value in *Plagiogramma staurophorum*. Fig 2 shows that in all growth forms except
287 motile epipsammon there were species (*Seminavis robusta*, *Fragilaria*. cf. *subsalina*, *P.*
288 *staurophorum*, *Brockmanniella brockmannii*) for which a low NPQ developed without DT
289 synthesis, while two motile epipsammon species (*Amphora* sp. and *Planothidium*
290 *delicatulum*) showed DT synthesis (0.17 ± 0.03 mol 100 mol Chl a^{-1}) without NPQ. All other
291 species showed a NPQ/DT relationship with an origin close to 0, as expected.

292

293 *Effect of high light acclimation on the NPQ and XC properties (Figs 3-4, Tables S8-S9)*

294 All species were grown under an E ($75 \mu\text{mol photons m}^{-2} \text{s}^{-1}$) roughly corresponding to the
295 mean E_k for the low E acclimated cells ($20 \mu\text{mol photons m}^{-2} \text{s}^{-1}$, Table 3). Only epipelon had
296 significantly higher growth rates at $75 \mu\text{mol photons m}^{-2} \text{s}^{-1}$. DD+DT significantly increased
297 with a factor 1.6-1.7 in epipelon and epipsammon, and 2.3 in tychoplankton. There was a
298 significant increase in DES at $75 \mu\text{mol photons m}^{-2} \text{s}^{-1}$ in all growth forms except in motile
299 epipsammon. The increase in DD+DT and DES at the higher light intensity was most
300 pronounced in tychoplankton and resulted in a pronounced, significant difference in both
301 parameters between tychoplankton and epipelon at this light intensity. The comparison of Chl
302 fluorescence yield and light curve parameters could only be performed for a selection of six
303 species (covering all growth forms) and is summarised in Fig. 4. As expected, the Chl *a*
304 content per cell decreased, roughly with a factor of 2 in all species (except *Navicula*
305 *phyllepta*). There was only a slight (up to about 10 %) decrease in F_v/F_m in all species,
306 illustrating the unstressed state of the cells (note that in *Seminavis robusta* and *Planothidium*
307 *delicatulum* this decrease was slightly significant). DES_m significantly increased in *S. robusta*
308 only. Together with the overall increase in DD+DT, this resulted in a significant increase in
309 DT_m (by a factor of 4) in this species, but also in *P. delicatulum* and *Plagiogrammopsis*
310 *vanheurckii*. The corresponding NPQ_m did not follow the same trend: it significantly

311 increased in all species (except for *P. delicatulum* and *Opephora* sp.) but only by a factor of
312 maximally 2. NPQ/DT remained low (0.2 to 0.5) in all species (and significantly decreased in
313 *Opephora* sp.). $E50_{NPQ}$ was significantly higher only in the non-motile epipsammic species
314 *Plagiogramma staurophorum*.

315

316 *Effect of 'planktonic' growth on the NPQ and XC properties of tychoplankton (Fig. 5, Table*
317 *S10)*

318 The three tychoplanktonic species were grown under 'planktonic' conditions (at 20 μmol
319 $\text{photons.m}^{-2}.\text{s}^{-1}$) for a comparison with growth under 'benthic' conditions. *Brockmaniella*
320 *brockmannii* responded most strongly to a switch from 'benthic' to 'planktonic' growth: it
321 showed a significantly lower growth rate and a higher DES and DES_m but a lower NPQ_m ,
322 suggesting photosynthetic stress and investment of additional DT in other processes than
323 NPQ. *Plagiogrammopsis vanheurckii* and *Cylindrotheca closterium* showed very little
324 change, apart from a significantly higher growth rate during planktonic growth in *P.*
325 *vanheurckii*, a slight decrease in NPQ/DT in *C. closterium*, and an increase in DES in both
326 species. The most pronounced and consistent change in tychoplankton thus concerned an
327 increase in DES when grown in suspension. Note that there is also an overall decrease in
328 rETR_m , but this decrease was just not significant ($p=0.08$).

329 **Discussion**

330 The present work constitutes the first comparative experimental study, using unialgal cultures
331 in standardized conditions, of fast regulatory photoprotective mechanisms in the four main
332 benthic diatom growth forms present in intertidal marine sediments (epipelon, motile and
333 non-motile epipsammon and tychoplankton). Because no sediment was added in our
334 experiments, motile diatoms were not able to position themselves in a light gradient, hence
335 effectively incapacitating their behavioural response. As the growth rate and photosynthetic
336 characteristics (main pigments, F_v/F_m , α , E_k , $rETR_m$) of the studied species were comparable
337 between the growth forms at $20 \mu\text{mol photons m}^{-2} \text{ s}^{-1}$, we were able to compare their purely
338 physiological light response.

339 Our study revealed a highly significant and pronounced difference in NPQ between the four
340 growth forms. NPQ was significantly lower in epipellic and tychoplanktonic than in
341 epipsammic species; differences in DES were only observed between epipellic and other forms
342 at lower light intensities. Within the epipsammon, NPQ capacity was significantly higher in
343 the non-motile than in the motile forms. As all growth forms included both small and large
344 species, the functional light response (NPQ capacity) apparently did not depend on biovolume
345 or the Chl *a* concentration per cell, as has also been observed *in situ* (Jesus *et al.*, 2009). The
346 absence of significant differences in PSII CET between growth forms underscores the
347 importance of NPQ as the main fast photoprotective process in intertidal benthic diatoms,
348 confirming earlier results for these organisms (Lavaud *et al.*, 2002) but in contrast with
349 planktonic diatoms (Lavaud *et al.*, 2002; Lavaud *et al.*, 2007). By analogy with previous
350 studies on planktonic diatoms (Dimier *et al.*, 2009; Lavaud *et al.*, 2007; Lavaud and Lepetit,
351 2013; Petrou *et al.*, 2011; Strzepek and Harrison, 2004), our data suggest that epipellic and
352 tychoplanktonic diatoms are adapted to a less fluctuating light climate and/or to a lower

353 average irradiance, and vice versa for epipsammic diatoms. This result fits well with the
354 ecology of these growth forms. Epipelon is not only more abundant in muddy cohesive
355 sediments where light penetration is more restricted than in sandy sediments (Paterson and
356 Hagerthey 2001; Cartaxana *et al.*, 2011), but, more importantly, their (micro-)migratory
357 behaviour allows positioning at the optimal irradiance in the vertical light gradient and rapid
358 escape from periodic excess light (Kromkamp *et al.*, 1998; Conn *et al.*, 2004; Consalvey *et*
359 *al.*, 2004; Serôdio *et al.*, 2006). This alleviates the need to invest in a strong physiological
360 capacity to respond to light stress as previously proposed (Jesus *et al.*, 2009; Cartaxana *et al.*,
361 2011), although the right balance between motility and physiology still remains essential (van
362 Leeuwe *et al.*, 2009; Perkins *et al.*, 2010b; Cartaxana *et al.*, 2011; Serôdio *et al.*, 2012).

363 Such balance is more crucial in the motile epipsammic species, which can move but have only
364 limited control over their immediate light environment as movement is restricted, usually
365 within the sphere of individual sand grains. As expected, they showed a significantly lower
366 NPQ and a higher $E_{50_{NPQ}}$ than non-motile epipsammon, which have no behavioural control
367 over their light environment. An alternative, but not exclusive, explanation could be related to
368 the difference in exopolysaccharide (EPS) secretion between motile and non-motile growth
369 forms. EPS secretion could work as an alternative electron sink under stressful conditions (i.e.
370 high light, nutrient limitation, etc.) in order to limit the over-reduction of the photosynthetic
371 machinery ('overflow' hypothesis; Staats *et al.*, 2000), alleviating the need for a strong NPQ.
372 However, EPS secretion is not as fast as NPQ (minutes/hours *vs.* seconds/minutes) and may
373 not be useful to the cells for responding to rapid light changes but only to cope with
374 prolonged high light exposure. Additionally, while the 'overflow' hypothesis is often
375 proposed (Underwood and Paterson, 2003; Stal, 2009), it was never clearly proven. A few
376 studies have shown a positive relationship between light intensity and EPS production

377 (Underwood, 2002; Wolfstein and Stal, 2002) but other studies have reported a negative
378 relation with light intensity and no relationship with nutrient limitation (Hanlon *et al.*, 2001;
379 Perkins *et al.*, 2006). To date there is no information on EPS production in different benthic
380 diatom growth forms, and only epipelagic species have been compared (Underwood and
381 Paterson, 2003), showing no clear relationship between light response and EPS secretion. To
382 our knowledge, there are no reports on a relationship between NPQ-XC capacity and EPS
383 production. Finally, tychoplankton typically alternates between resuspension in a highly
384 turbid shallow water column at high tide and deposition and burial in the upper sediment
385 layers of muddy sediments at low tide (deposition in sandy sediments does not occur due to
386 the intense hydrodynamic disturbance in these sediments). As such, the tychoplankton
387 resembles planktonic diatoms adapted to subtle light fluctuations and/or on average low
388 irradiance (Bailleul *et al.*, 2010; Lavaud and Lepetit, 2013).

389 The reason for the NPQ differences between epipelagic and epipsammonic can be explained by
390 its main control: the XC dynamics. Previous *in situ* studies reported a consistently stronger
391 DES under light stress in epipsammonic than in epipelagic diatom communities (i.e. in sandy vs.
392 muddy sediments) and related growth form with differential (behavioural vs. physiological)
393 photoregulatory strategies (Jesus *et al.*, 2009; Cartaxana *et al.*, 2011). As recently shown, a
394 high NPQ is supported by the strong effective involvement of DT which first depends both on
395 a high DD+DT content and a high DES (Lavaud and Lepetit, 2013). The slope of the
396 NPQ/DT relationship has been proposed as a good indicator of light climate adaptation: the
397 higher the NPQ/DT slope, the better the adaptation to a highly fluctuating and/or on average
398 high light climate (Dimier *et al.*, 2009; Lavaud and Lepetit, 2013). All epipsammonic species,
399 and especially the non-motile ones, showed XC parameter values which are characteristic for
400 a high NPQ capacity, viz. a higher DD+DT content and DT_m which was 2x higher than in

401 epipelon. Non-motile epipsammon also tended to show a higher efficiency in promoting NPQ
402 (NPQ/DT), but this difference was not significant due to high intra-group variability.

403 Within the epipsammon, NPQ is clearly more efficient in non-motile than motile epipsammic
404 species. In motile epipsammon, the discrepancy between $E_{50_{NPQ}}$ and E_k is more pronounced
405 than in non-motile forms: while there is no significant difference in E_k between both growth
406 forms, $E_{50_{NPQ}}$ is significantly higher in the motile growth forms. This suggests a weaker
407 relationship between NPQ development and photochemistry in the latter group, with slower
408 NPQ development with increasing E. Remarkably, $E_{50_{DT}}$ does not significantly differ
409 between both growth forms, and the significantly higher initial induction of DT synthesis
410 (n_{DT}) but not NPQ (n_{NPQ}) in the motile group, together with the fact that some representatives
411 of this group show DT synthesis without NPQ, suggests that either DT is less or not involved
412 in NPQ development, or that the light-dependent built-up of the transthylakoidal proton
413 gradient (which is involved in both the activation of the DD de-epoxidase and the molecular
414 control of NPQ) and the onset of NPQ are uncoupled (Lavaud *et al.*, 2012; Lavaud and
415 Lepetit, 2013). Our observations thus suggest that in contrast to the non-motile group, motile
416 epipsammic species rely more on a behavioural response (motility) and/or involve DT in
417 other photoprotective processes such as the prevention of lipid peroxidation by reactive
418 oxygen species (ROS) (Lepetit *et al.*, 2010). The increase in $E_{50_{NPQ}}$ in the non-motile
419 epipsammic species *Plagiogramma staurophorum* during a shift to higher light illustrates the
420 ability to physiologically modulate the NPQ *vs.* E development kinetics to its light
421 environment in contrast to motile epipsammon, epipelon and tychoplankton.

422 The influence of DT on the inter-group/species NPQ differences was further investigated by
423 the acclimation to higher light ($75 \mu\text{mol photons m}^{-2} \text{s}^{-1}$, close to the mean E_k for cells
424 acclimated to $20 \mu\text{mol photons m}^{-2} \text{s}^{-1}$). High light exposure is known to induce constitutive

425 DT synthesis (Schumann *et al.*, 2007) and in field conditions, DT is usually even present in
426 significant amounts in cells adapted to low/moderate light (Jesus *et al.*, 2009; van Leeuwe *et*
427 *al.*, 2009; Chevalier *et al.*, 2010; Cartaxana *et al.*, 2011). Acclimation to higher light resulted
428 in a significant increase in XC pigments (DD+DT) and DES in most growth forms,
429 suggesting that although epipelon uses behavioural photoprotection, the XC is still important
430 (cf. above). NPQ_m increased in most of the species examined, mainly due to a higher DT_m
431 resulting from a higher DD+DT rather than a higher DES_m. The discrepancy between DES_m
432 and NPQ_m as well as the low NPQ/DT may be due to the fact that the additional DT primarily
433 served in the prevention of lipid peroxidation rather than in NPQ as previously reported in
434 high light acclimated diatoms (see also above).

435 While under low light conditions, the growth, photosynthetic and steady-state light-response
436 features of tycho plankton were similar to those of epipellic diatoms (i.e. low NPQ, NPQ_m and
437 DT_m), their dynamic light response was significantly different, i.e. higher E50_{NPQ}.
438 Surprisingly, E50_{NPQ} was beyond the natural light maximum (2000-2500 μmol photons m⁻² s⁻¹
439 ¹) illustrating the inability of tycho plankton to strongly and/or continuously develop NPQ in
440 the environmental high light range (a situation also encountered in one epipellic species:
441 *Navicula phyllepta*). In contrast, its low n_{NPQ} supported a relatively strong onset of NPQ at
442 low Es. Both E50_{DT} and n_{DT} were correspondingly high and low, respectively (and
443 significantly different from epipelon for n_{DT}), although E50_{DT} was much lower than E50_{NPQ}
444 suggesting a discrepancy between DT synthesis and NPQ development (cf. above). The
445 response of tycho plankton to higher light was much more pronounced, with the strongest
446 increase in XC pigments and DES of all growth forms. However, the NPQ_m and DT_m data
447 (only available however for one representative species, *Plagiogrammopsis vanheurckii*) did
448 not show a similar response, with DT_m showing a more pronounced increase than NPQ_m,

449 suggesting that NPQ development was low and that DT may have mainly been involved in
450 other processes than NPQ. For most parameters, the response of the tychoplankton species to
451 growth in suspension ('planktonic' growth) was limited and largely species-specific, except
452 for a general increase in DES and a decrease (albeit just non-significant) in $rETR_m$. These data
453 suggest that representatives of the tychoplanktonic growth form are well-adapted to their
454 amphibious life style, which is characterized by an on average low irradiance (MacIntyre *et*
455 *al.*, 1996). In contrast, epipellic species do not grow well in suspended, turbulent conditions (J.
456 Lavaud, pers. observation).

457 Our study for the first time shows that intertidal benthic diatoms display growth form specific
458 variation in fast regulatory physiological mechanisms for photoprotective capacity (NPQ and
459 the XC), which mirrors their behavioural light response. In epipellic motile diatoms,
460 exclusively belonging to the raphid pennate clade, the physiological response is not well
461 developed, as these diatoms appear to largely rely on motility to control their immediate light
462 environment. In the motile epipsammon however the physiological response remains essential
463 because their movement is restricted to the sphere of individual sand grains. The evolution of
464 the raphe system, the hallmark synapomorphy of the raphid pennate diatom clade which
465 enables locomotion, has therefore been essential for the colonization of intertidal sediments
466 by not only migratory epipellic biofilms but also motile epipsammon. In contrast, NPQ and
467 XC capacity is high in non-motile araphid pennate diatoms which passively have to abide
468 often pronounced variations in the intertidal light climate. Tychoplanktonic diatoms, which
469 alternate between high tide resuspension in a turbulent and turbid water column, and low tide
470 deposition in muddy sediments, appear to be adapted to an on average low light environment,
471 with low NPQ and XC capacity.

472 While we made no formal analysis of the relationship between functional and phylogenetic
473 diversity, it is obvious that despite the fact that a behavioural photoprotective response
474 (motility) is restricted to the raphid pennate diatom clade, differences in the studied
475 physiological traits are more strongly driven by growth form than phylogenetic relatedness.
476 For example, the epipsammic species *Biremis lucens*, despite being a raphid pennate species,
477 has a non-motile growth form, and shows a NPQ capacity which is more similar to non-motile
478 epipsammon than to the (phylogenetically more closely related) motile epipsammon and
479 epipelon. Likewise, photophysiological features of pennate raphid (*Cylindrotheca closterium*)
480 and centric (*Plagiogrammopsis vanheurckii* and *Brockmanniella brockmannii*) tychoplankton
481 species were similar as reported before in planktonic centric/pennate species (Lavaud *et al.*,
482 2004). Raphid pennate diatoms which have colonized an epipsammic or tychoplanktonic
483 niche thus display a reverse evolutionary trade-off switch towards a much more performant
484 physiological response. Our observations thus suggest that photoprotective capacity in
485 diatoms is a highly adaptive trait which is to a certain degree constrained by clade-specific
486 evolutionary innovations (the evolution of the raphe system and hence a behavioural
487 response) but also, and more importantly, by growth form, which ultimately defines the
488 balance between the physiological and behavioural photoprotective response in these
489 organisms. Such differential adaptation is of primary importance for the regulation of the
490 photosynthetic productivity *vs.* light, as has been demonstrated before in planktonic diatoms,
491 where the photochemical *vs.* the photoprotective energy allocation as a function of light is
492 drastically different in species adapted to a fluctuating *vs.* a more stable light environment
493 (Wagner *et al.*, 2006; Lavaud *et al.*, 2007; Petrou *et al.*, 2011; Lavaud and Lepetit, 2013).
494 However, unlike in planktonic environments, the trade-off between a physiological and
495 behavioural response in benthic diatoms allows local co-existence of different growth forms
496 under the same overall light environment.

497

498 **Acknowledgements**

499 The authors acknowledge the Centre National de la Recherche Scientifique-CNRS, the
500 University of La Rochelle-ULR, the Contrat Plant Etat Région-CPER 'Littoral', the Region
501 Poitou-Charentes, the Deutscher Akademischer Austausch Dienst-DAAD, the Research
502 Foundation Flanders (FWO project G.0222.09N), Ghent University (BOF-GOA 01G01911)
503 and the Egide/Campus France-PHC Tournesol (n°28992UA) exchange program for their
504 financial support.

505

506 **The authors formally declare that no conflict of interest exists.**

507

508 **Supplementary information is available at The ISME Journal's website**

509

510

511 **References**

512 Admiraal W. (1984). The ecology of estuarine sediment inhabiting diatoms. *Prog Phycol Res*
513 **3**: 269-314.

514 Armbrust EV. (2009). The life of diatoms in the world's oceans. *Nature* **459**: 185-192.

515 Bailleul B, Rogato A, de Martino A, Coesel S, Cardol P, Bowler C *et al.* (2010). An atypical
516 member of the light-harvesting complex stress-related protein family modulates diatom
517 responses to light. *Proc Natl Acad Sci USA* **107**: 18214-18219.

518 Barton AD, Pershing AJ, Lichtman E, Record NR, Edwards KF, Finkel ZV *et al.* (2013). The
519 biogeography of marine plankton traits. *Ecol Lett* **16**: 522-534.

520 Brunet C, Lavaud J. (2010). Can the xanthophyll cycle help extract the essence of the
521 microalgal functional response to a variable light environment ? *J Plankton Res* **32**: 1609-
522 1617.

523 Cartaxana P, Ruivo M, Hubas C, Davidson I, Serôdio J, Jesus B. (2011). Physiological versus
524 behavioral photoprotection in intertidal epipellic and epipsammic benthic diatom communities.
525 *J Exp Mar Biol Ecol* **405**: 120-127.

526 Chevalier EM, Gévaert F, Créach A. (2010). In situ photosynthetic activity and xanthophylls
527 cycle development of undisturbed microphytobenthos in an intertidal mudflat. *J Exp Mar Biol*
528 *Ecol* **385**: 44-49.

529 Coelho H, Vieira S, Serôdio J. (2011). Endogenous versus environmental control of vertical
530 migration by intertidal benthic microalgae. *Eur J Phycol* **46**: 271-281.

531 Conn SA, Bahena M, Davis JT, Ragland RL, Rauschenberg CD, Smith BJ. (2004).
532 Characterisation of the diatom photophobic response to high irradiance *Diatom Res* **19**: 167-
533 179.

534 Consalvey M, Paterson DM, Underwood GJC. (2004). The ups and downs of life in a benthic
535 biofilm: migration of benthic diatoms. *Diatom Res* **19**: 181-202.

536 Depauw FA, Rogato A, d'Alcala MR, Falciatore A. (2012). Exploring the molecular basis of
537 responses to light in marine diatoms. *J Exp Bot* **63**: 1575-1591.

538 Dimier C, Corato F, Tramontano F, Brunet C. (2007). Photoprotective capacity as functional
539 trait in planktonic algae: relationship between xanthophyll cycle and ecological characteristics
540 in three diatoms. *J Phycol* **43**: 937-947.

541 Dimier C, Giovanni S, Ferdinando T, Brunet C. (2009). Comparative ecophysiology of the
542 xanthophyll cycle in six marine phytoplanktonic species. *Protist* **160**: 397-411.

543 Edwards KF, Litchman E, Klausmeier CA. (2013). Functional traits explain phytoplankton
544 community structure and seasonal dynamics in a marine ecosystem. *Ecol Lett* **16**: 56-63.

545 Eilers PHC, Peeters JCH. (1988). A model for the relationship between light intensity and the
546 rate of photosynthesis in phytoplankton. *Ecol Model* **42**: 199-215.

547 Goss R, Jakob T. (2010). Regulation and function of xanthophyll cycle-dependent
548 photoprotection in algae. *Photosynth Res* **106**: 103-122.

549 Gottschalk S, Kahlert M. (2012). Shifts in taxonomical and guild composition of littoral
550 diatom assemblages along environmental gradients. *Hydrobiologia* **694**: 41-56.

551 Hamels I, Sabbe K, Muylaert K, Barranguet C, Lucas C, Herman P, Vyverman W. (1998)
552 Organisation of microbenthic communities in intertidal estuarine flats, a case study from the
553 Molenplaat (Westerschelde estuary, The Netherlands). *Europ J Protistol* **34**: 308-320.

554 Haubois A-G, Sylvestre F, Guarini J-M, Richard P, Blanchard GF. (2005). Spatio-temporal
555 structure of the epipellic diatom assemblage from an intertidal mudflat in Marennes-Oleron
556 Bay, France. *Est Coast Shelf Sci* **64**: 385-394.

557 Herlory O, Guarini J-M, Richard P, Blanchard GF. (2004). Microstructure of
558 microphytobenthic biofilm and its spatio-temporal dynamics in an intertidal mudflat
559 (Aiguillon Bay, France). *Mar Ecol Prog Ser* **282**: 33-44.

560 Hanlon ARM, Bellinger B, Haynes K, Xiao G, Hofmann TA, Gretz MR, Ball AS, Osborn
561 AM, Underwood GJC. (2006) Dynamics of extracellular polymeric substance (EPS)
562 production and loss in an estuarine, diatom-dominated, microalgal biofilm over a tidal
563 emersion–immersion period. *Limnol Oceanogr* **51**: 79-93.

564 Hillebrand C, Durselen CD, Kirschtel D, Pollinger U, Zohary T. (1999). Biovolume
565 calculation for pelagic and benthic microalgae. *J Phycol* **35**: 403-424.

566 Huisman J, Johansson AM, Folmer EO, Weissing FJ. (2001). Towards a solution of the
567 plankton paradox: the importance of physiology and life history. *Ecol Lett* **4**: 408-411.

568 Jakob T, Goss R, Wilhelm C. (1999). Activation of diadinoxanthin de-epoxidase due to a
569 chlororespiratory proton gradient in the dark in the diatom *Phaeodactylum tricornutum*. *Plant*
570 *Biol* **1**: 76-82.

571 Jeffrey SW, Humphrey GR. (1975). New spectrophotometric equations for determining
572 chlorophylls a, b, c1 and c2 in higher plants, algae and natural phytoplankton. *Biochem*
573 *Physiol Pflanzen Bd* **167**: 191-194.

574 Jesus BM, Brotas V, Ribeiro L, Mendes CR, Cartaxana P, Paterson DM. (2009). Adaptations
575 of microphytobenthos assemblages to sediment type and tidal position. *Cont Shelf Res* **29**:
576 1624-1634.

577 Jørgensen E, Pedersen AR. (1998). How to obtain those nasty standard errors from
578 transformed data - and why they should not be used. In: 7 BRU-Ir (ed). Danish Institute of
579 Agricultural Sciences. p 20.

580 Key T, McCarthy A, Campbell DA, Six C, Roy S, Finkel ZV. (2010). Cell size trade-offs
581 govern light exploitation strategies in marine phytoplankton. *Environ Microbiol* **12**: 95-104.

582 Kooistra WHCF, Gersonde R, Medlin LK, Mann DG. (2007). The origin and the evolution of
583 the diatoms: Their adaptation to a planktonic existence. In: Falkowski PG, Knoll AH (eds).
584 *Evolution of Primary Producers in the Sea*. Elsevier Academic Press: Burlington. pp 207-249.

585 Kromkamp J, Barranguet C, Peene J. (1998). Determination of microphytobenthos PSII
586 quantum efficiency and photosynthetic activity by means of variable chlorophyll
587 fluorescence. *Mar Ecol Prog Ser* **162**: 45-55.

588 Larson CA, Passy SI. (2012). Taxonomic and functional composition of the algal benthos
589 exhibits similar successional trends in response to nutrient supply and current velocity. *FEMS*
590 *Microbiol Ecol* **80**: 352-360.

591 Lavaud J, van Gorkom HJ, Etienne A-L. (2002). Photosystem II electron transfer cycle and
592 chlororespiration in planktonic diatoms. *Photosynth Res* **74**: 51-59.

593 Lavaud J, Rousseau B, Etienne A-L. (2004). General features of photoprotection by energy
594 dissipation in planktonic diatoms (Bacillariophyceae). *J Phycol* **40**: 130-137.

595 Lavaud J (2007). Fast regulation of photosynthesis in diatoms: Mechanisms, evolution and
596 ecophysiology. *Funct Plant Sci Biotech* **267**: 267-287.

597 Lavaud J, Strzepek RF, Kroth PG. (2007). Photoprotection capacity differs among diatoms:
598 Possible consequences on the spatial distribution of diatoms related to fluctuations in the
599 underwater light climate. *Limnol Oceanogr* **52**: 1188-1194.

600 Lavaud J, Materna AC, Sturm S, Vugrinec S, Kroth PG. (2012). Silencing of the violaxanthin
601 de-epoxidase gene in the diatom *Phaeodactylum tricornutum* reduces diatoxanthin synthesis
602 and non-photochemical quenching. *PLoS ONE* **7**: e36806.

603 Lavaud J, Lepetit B. (2013). An explanation for the inter-species variability of the
604 photoprotective non-photochemical chlorophyll fluorescence quenching in diatoms. *Biochim*
605 *Biophys Acta* **1827**: 294-302.

606 Lepetit B, Volke D, Gilbert M, Wilhelm C, Goss R. (2010). Evidence for the existence of one
607 antenna-associated, lipid-dissolved and two protein-bound pools of diadinoxanthin cycle
608 pigments in diatoms. *Plant Physiol* **154**: 1905-1920.

609 Lepetit B, Goss R, Jakob T, Wilhelm C. (2012). Molecular dynamics of the diatom thylakoid
610 membrane under different light conditions. *Photosynth Res* **111**: 245-257.

611 Lepetit B, Sturm S, Rogato A, Gruber A, Sachse M, Falciatore A *et al.* (2013). High light
612 acclimation in the secondary plastids containing diatom *Phaeodactylum tricornutum* is
613 triggered by the redox state of the plastoquinone pool. *Plant Physiol* **161**: 853-865.

614 Litchman E, Klausmeier CA. (2008). Trait-based community ecology of phytoplankton. *Ann*
615 *Rev Ecol Evol Syst* **39**: 615-639.

616 MacIntyre HL, Geider JR, Miller DC. (1996). Microphytobenthos: The ecological role of the
617 'secret garden' of unvegetated, shallow-water marine habitats. I. Distribution, abundance and
618 primary production. *Estuaries* **19**: 186-201.

619 Méléder V, Rincé Y, Barillé L, Gaudin P, Rosa P. (2007). Spatiotemporal changes in
620 microphytobenthos assemblages in a macrotidal flat (Bourgneuf Bay, France). *J Phycol* **43**:
621 1177-1190.

622 Mouget JL, Perkins R, Consalvey M, Lefebvre S. (2008). Migration or photoacclimation to
623 prevent high irradiance and UV-B damage in marine microphytobenthic communities. *Aquat*
624 *Microb. Ecol.* **52**: 223-232.

625 Paterson DM, Hagerthey SE. (2001). Microphytobenthos in contrasting coastal ecosystems:
626 Biology and dynamics. In: Reise K. (ed). *Ecological Comparisons of Sedimentary Shores*.
627 Springer-Verlag: Berlin Heidelberg. pp 106-125.

628 Perkins RG, Underwood GJC, Brotas V, Snow GC, Jesus B, Ribeiro L. (2001) Response of
629 microphytobenthos to light: primary production and carbohydrate allocation over an emersion
630 period. *Mar Ecol Prog Ser* **223**: 101-112.

631 Perkins RG, Mouget J-L, Lefebvre S, Lavaud J. (2006). Light response curve methodology
632 and possible implications in the application of chlorophyll fluorescence to benthic diatoms.
633 *Mar Biol* **149**: 703-712.

634 Perkins RG, Kromkamp JC, Serôdio J, Lavaud J, Jesus BM, Mouget J-L *et al.* (2010a). The
635 Application of variable chlorophyll fluorescence to microphytobenthic biofilms. In: Suggett
636 DJ, Prášil O, Borowitzka MA. (eds). *Chlorophyll a Fluorescence in Aquatic Sciences:*
637 *Methods and Applications*. Springer Netherlands. pp 237-275.

638 Perkins RG, Lavaud J, Serôdio J, Mouget J-L, Cartaxana P, Rosa P *et al.* (2010b). Vertical
639 cell movement is a primary response of intertidal benthic biofilms to increasing light dose.
640 *Mar Ecol Prog Ser* **416**: 93-103.

641 Petrou K, Doblin MA, Ralph PJ. (2011). Heterogeneity in the photoprotective capacity of
642 three Antarctic diatoms during short-term changes in salinity and temperature. *Mar Biol* **158**:
643 1029-1041.

644 Ribeiro L, Brotas V, Rincé Y, Jesus BM. (2013). Structure and diversity of intertidal benthic
645 diatom assemblages in contrasting shores: A case study from the Tagus estuary. *J Phycol.*

646 Roy S, Llewellyn CA, Skarstad Egeland E, Johnsen G. (2011) *Phytoplankton Pigments-*
647 *Characterization, Chemotaxonomy and Applications in Oceanography*, Cambridge
648 *Environmental Chemistry Series*, Cambridge University Press, Cambridge, UK, 845 pp.

649 Underwood GJC. (2002). Adaptation of tropical marine microphytobenthic assemblages
650 along a gradient for light and nutrient availability in Suva Lagoon, Fidji. *Eur J Phycol* **37**:
651 449-462.

652 Underwood GJC, Paterson DM. (2003). The importance of extracellular carbohydrate
653 production by marine epipelagic diatoms. *Adv Bot Res* **40**: 183-240.

654 Sabbe K. (1993). Short-term fluctuations in benthic diatom numbers on an intertidal sandflat
655 in the Westerschelde estuary (Zeeland, The Netherlands). *Hydrobiologia* **269-270**: 275-284.

656 Sabbe K, Witkowski A, Vyverman W. (1995). Taxonomy, morphology and ecology of
657 *Biremis lucens* comb. nov. (Bacillariophyta): a brackish-marine, benthic diatom species
658 comprising different morphological types. *Bot Mar* **38**: 379-391.

659 Sabbe K, Vanellander B, Ribeiro L, Witkowski A, Muylaert K, Vyverman W. (2010). A new
660 genus, *Pierrecomperia* gen. nov., a new species and two new combinations in the marine
661 diatom family *Cymatosiraceae*. *Vie et Milieu* **60**: 243-256.

662 Saburova MA, Polikarpov IG. (2003). Diatom activity within soft sediments: behavioural and
663 physiological processes. *Mar Ecol Prog Ser* **251**: 115-126.

664 Schumann A, Goss R, Jakob T, Wilhelm C. (2007). Investigation of the quenching efficiency
665 of diatoxanthin in cells of *Phaeodactylum tricornutum* (Bacillariophyceae) with different pool
666 sizes of xanthophyll cycle pigments. *Phycologia* **46**: 113-117.

667 Schwaderer AS, Yoshiyama K, de Tezanos Pinto P, Swenson NG, Klausmeier CA, Litchman
668 E. (2011). Eco-evolutionary differences in light utilization traits and distributions of
669 freshwater phytoplankton. *Limnol Oceanogr* **56**: 589-598.

670 Serôdio J, Cruz S, Vieira S, Brotas V. (2005). Non-photochemical quenching of chlorophyll
671 fluorescence and operation of the xanthophyll cycle in estuarine microphytobenthos. *J Exp*
672 *Mar Biol Ecol* **326**: 157-169.

673 Serôdio J, Coelho H, Vieira S, Cruz S. (2006). Microphytobenthos vertical migratory
674 photoresponse as characterised by light-response curves of surface biomass. *Est Coast Shelf*
675 *Sci* **68**: 547-556.

676 Serôdio J, Vieira S, Cruz S. (2008). Photosynthetic activity, photoprotection and
677 photoinhibition in intertidal microphytobenthos as studied in situ using variable chlorophyll
678 fluorescence. *Cont Shelf Res* **28**: 1363-1375.

679 Serôdio J, Lavaud J. (2011). A model for describing the light response of the
680 nonphotochemical quenching of chlorophyll fluorescence. *Photosynth Res* **108**: 61-76.

681 Serôdio J, Ezequiel J, Barnett A, Mouget J-L, Méléder V, Laviale M *et al.* (2012). Efficiency
682 of photoprotection in microphytobenthos: Role of vertical migration and the xanthophyll
683 cycle against photoinhibition. *Aquat Microb Ecol* **67**: 161-175.

684 Staats N, Stal LJ, de Winder B., Mur LR. (2000). Oxygenic photosynthesis as driving process
685 in exopolysaccharide production in benthic diatoms. *Mar Ecol Prog Ser* **193**: 261-269.

686 Stal LJ. (2009). Microphytobenthos as a biogeomorphological force in intertidal sediment
687 stabilization. *Ecol Eng* **36**: 236-245.

688 Strzepek RF, Harrison PJ. (2004). Photosynthetic architecture differs in coastal and oceanic
689 diatoms. *Nature* **431**: 689-692.

690 Underwood GJC, Kromkamp J. (1999). Primary production by phytoplankton and
691 microphytobenthos in estuaries. In: Nedwell DB, Raffaelli DG. (eds). *Adv Ecol Res.*
692 Academic Press. pp 93-153.

693 van Leeuwe MA, Brotas V, Consalvey M, Forster RM, Gillespie D, Jesus B *et al.* (2009).
694 Photacclimation in microphytobenthos and the role of the xanthophylls pigments. *Eur J*
695 *Phycol* **43**: 123-132.

696 Wagner H, Jakob T, Wilhelm C. (2006). Balancing the energy flow from captured light to
697 biomass under fluctuating light conditions. *New Phytol* **169**: 95-108.

698 Wolstein K, Stal LJ. (2002). Production of extracellular polymeric substances (EPS) by bethic
699 diatoms: effect of irradiance and temperature. *Mar Ecol Prog Ser* **236**: 13-22.

700 Wu H, Roy S, Alami M, Green BR, Campbell AD. (2012). Photosystem II photoinactivation,
701 repair, and protection in marine centric diatoms. *Plant Physiol* **160**: 464-476.

702

703 **Titles and legends to figures and tables.**

704

705 **Figure 1.** Non-photochemical quenching of Chl fluorescence (NPQ) (A), de-epoxidation state
706 of the diadinoxanthin (DD) to diatoxanthin (DT) [DES = DT / (DD + DT) x 100] (B), and DT
707 content (C) as a function of light intensity (E from darkness to 1950 $\mu\text{mol photons m}^{-2} \text{ s}^{-1}$
708 which is equivalent to full sunlight in the field) measured during Non-Sequential Light
709 Curves (NSLCs) in the four benthic diatom growth forms (EPM-NM, epipsammon non-
710 motile, EPM-M, epipsammon motile; EPL, epipelon; TYCHO, thychoplankton). Cells were
711 grown at 20 $\mu\text{mol photons m}^{-2} \text{ s}^{-1}$. The NPQ-E curves for the individual species can be found
712 in Fig. S2. Values are estimated least squares means \pm estimated standard errors (PROC
713 MIXED procedure).

714

715 **Figure 2.** Non-photochemical quenching of Chl fluorescence (NPQ) as a function of the
716 amount of diatoxanthin (DT) measured during Non-Sequential Light Curves (NSLCs) in the
717 five species of epipelon (EPL) (A), the four species of motile epipsammon (EPM-M) (B), the
718 three species of thychoplankton (TYCHO) (C), and the three species of non-motile
719 epipsammon (EPM-NM) (D). Cells were grown at 20 $\mu\text{mol photons m}^{-2} \text{ s}^{-1}$. The full names
720 and classification of all species is listed in Table 1.

721

722 **Figure 3.** Growth rate (μ) (A), diadinoxanthin (DD) + diatoxanthin (DT) content (B) and de-
723 epoxidation state of DD to DT [DES = (DT / DD+DT x 100)] (C) in the four benthic diatom
724 growth forms (EPM-NM, epipsammon non-motile, EPM-M, epipsammon motile; EPL,
725 epipelon motile; TYCHO, thychoplankton) for cells grown at light intensities of 20 and 75
726 $\mu\text{mol photons m}^{-2} \text{ s}^{-1}$ respectively. All parameters were measured on cells in exponential
727 growth and sampled 2 h after the onset of light; growth conditions were 16 h light:8 h dark,

728 20°C. The values for all species in 20 and 75 $\mu\text{mol photons m}^{-2} \text{s}^{-1}$ conditions are found in
729 Tables S2 and S8, respectively. Values are estimated least squares means \pm estimated standard
730 errors (PROC MIXED procedure).

731

732 **Figure 4.** Comparison of photosynthetic, non-photochemical quenching of Chl fluorescence
733 (NPQ) and xanthophyll cycle (XC) parameters measured in diatom species representative of
734 the four benthic diatom growth forms grown at light intensities of 20 and 75 $\mu\text{mol photons m}^{-2} \text{s}^{-1}$
735 respectively. For each parameter the ratio of the values obtained at 75 and 20 μmol
736 $\text{photons m}^{-2} \text{s}^{-1} - 1$ was calculated (i.e. the 0 line is equal to a 75/20 ratio = 1 which is
737 equivalent to no change of values between light intensities). Significant changes between both
738 light intensities are indicated with an asterisk. The values used for the 20 and the 75 μmol
739 $\text{photons m}^{-2} \text{s}^{-1}$ conditions can be found in Tables S2/S4 and S8/S9 respectively.

740

741 **Figure 5.** Comparison of growth, photosynthetic, pigment, non-photochemical quenching of
742 Chl fluorescence (NPQ) and xanthophyll cycle (XC) parameters measured in the three
743 tychoplankton diatom species in ‘benthic’ and ‘planktonic’ conditions. For each parameter the
744 ratio of the values obtained under benthic and planktonic conditions – 1 was calculated (i.e.
745 the 0 line is equal to a planktonic/benthic ratio = 1 which is equivalent to no change of values
746 between ‘benthic’ and ‘planktonic’ conditions). Chl *a* per cell (in pg cell⁻¹) and growth rates
747 (in day⁻¹) were measured on cells in exponential growth phase sampled 2 h after the onset of
748 light; growth conditions were 20 $\mu\text{mol photons m}^{-2} \text{s}^{-1}$, 16 h light:8 h dark, 20°C. Significant
749 changes between both light intensities are indicated with an asterisk. The values used for the
750 ‘benthic’ and ‘planktonic’ growth conditions can be found in Tables S2/S4 and S10
751 respectively.

752

753

754 **Table 1: List of the fifteen diatom species used in this study with their growth form**
755 **classification, collection number, origin and average biovolume.**

756 Abbreviations: NCC, Nantes Culture Collection-France ; UTCC, University of Toronto
757 Culture Collection of Algae and Cyanobacteria-Canada (now the Canadian Phycological
758 Culture Collection-CPCC); CCY, Culture Collection Yerseke-The Netherlands; DCG: BCCM
759 (Belgian Coordinated Collections of Microorganisms) Diatom Culture Collection hosted by
760 Laboratory for Protistology & Aquatic Ecology, Ghent University, Belgium ; n.d. not
761 determined.

762

763 **Table 2: Photophysiological parameters used in this study, their photophysiological**
764 **meaning and measurement method and conditions.** Abbreviations: Chl, chlorophyll; DD,
765 diadinoxanthin; DT, diatoxanthin; E, light intensity; NSLCs, Non-Sequential Light Curves;
766 PSII, photosystem II; RLCs, Rapid Light Curves. See the Materials and Methods section for
767 further details.

768

769 **Table 3: Growth rate, pigment content and photosynthetic properties of the four growth**
770 **forms of benthic diatoms.** All parameters were measured on cells in exponential growth
771 phase sampled 2 h after the onset of light. Growth conditions were $20 \mu\text{mol photons m}^{-2} \text{s}^{-1}$,
772 16 h light:8 h dark, 20°C. Abbreviations: EPL, epipelon; EPM-M, motile epipsammon; EPM-
773 NM, non-motile epipsammon; TYCHO, tychoplankton. μ , growth rate (day^{-1}); Chl $a \text{ cell}^{-1}$,
774 content of chlorophyll a (in pg) per diatom cell; other pigments are expressed in mol 100 mol.
775 Chl a^{-1} : Chl, chlorophyll; Fx, fucoxanthin; β -car, β -carotene; DD, diadinoxanthin; DT,
776 diatoxanthin. Definitions and conditions of measurement of all parameters are listed in Table

777 2. The values for the individual species can be found in Table S2. Values are least squares
778 means estimates and estimated standard errors (PROC MIXED procedure).

779

780 **Table 4: Non-photochemical quenching (NPQ) and xanthophyll cycle (XC) properties of**
781 **the four growth forms of benthic diatoms.** Abbreviations: EPL, epipelon; EPM-M, motile
782 epipsammon; EPM-NM, non-motile epipsammon; TYCHO, tychoplankton. Definitions and
783 conditions of measurement of all parameters are listed in Table 2. The values for the
784 individual species can be found in Tables S4. Values are least squares means estimates and
785 estimated standard errors (PROC MIXED procedure).

786

787

Figure 1

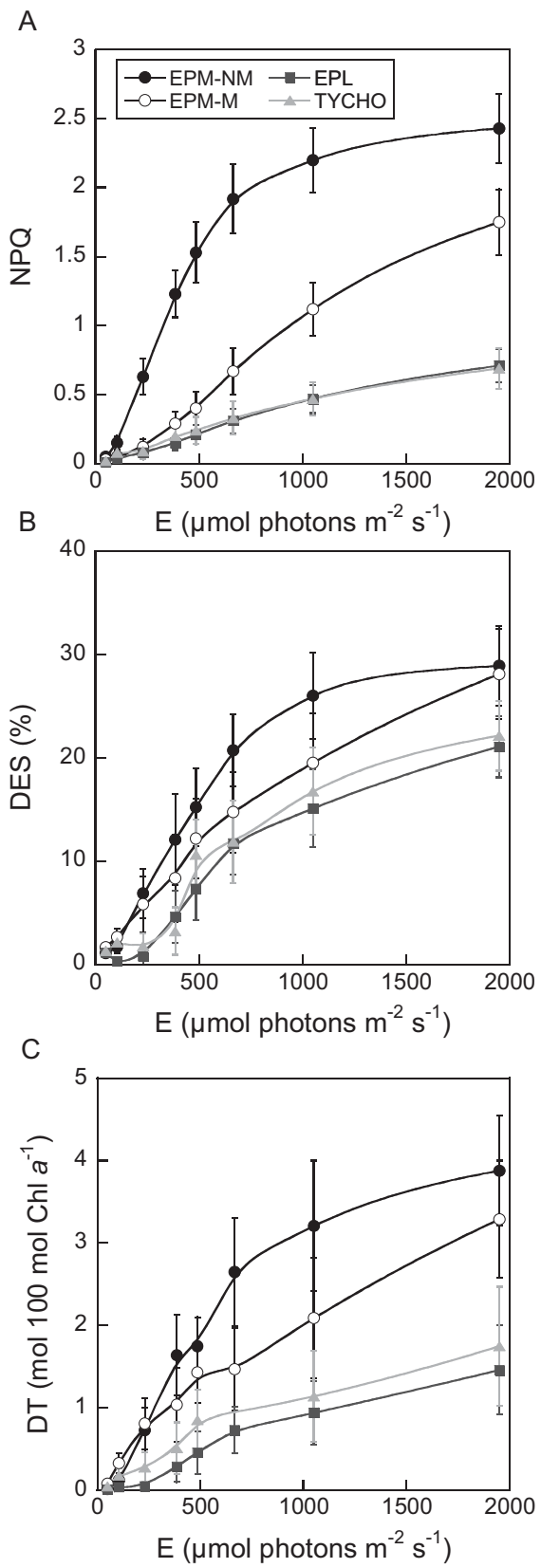


Figure 2

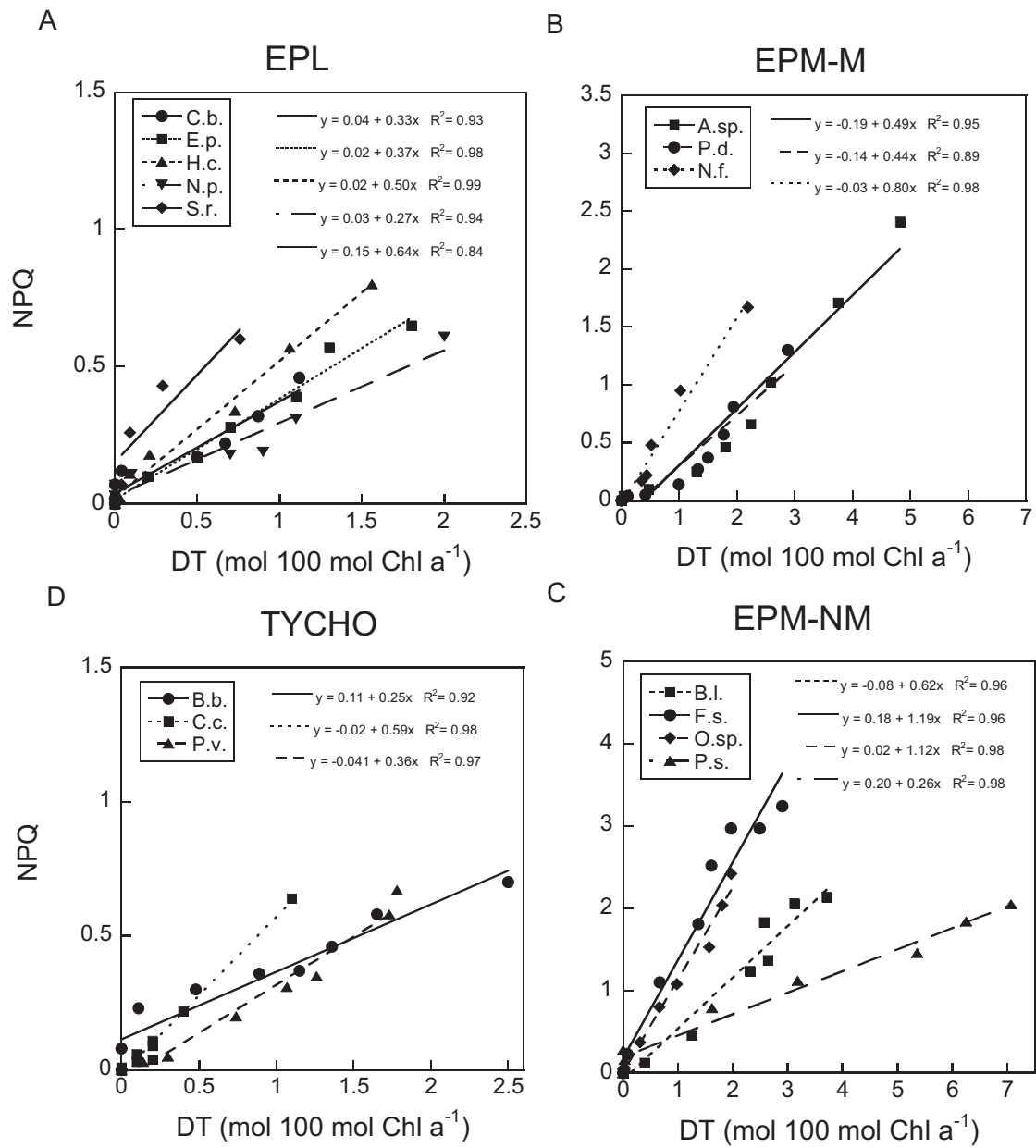


Figure 3

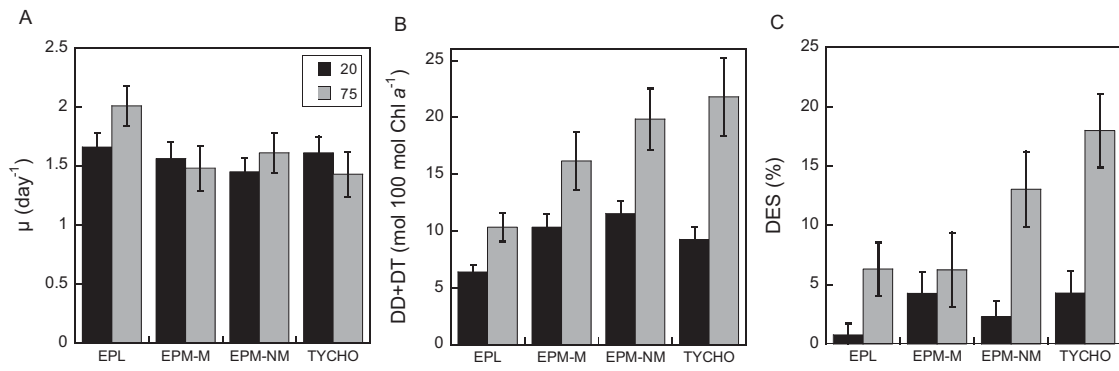


Figure 4

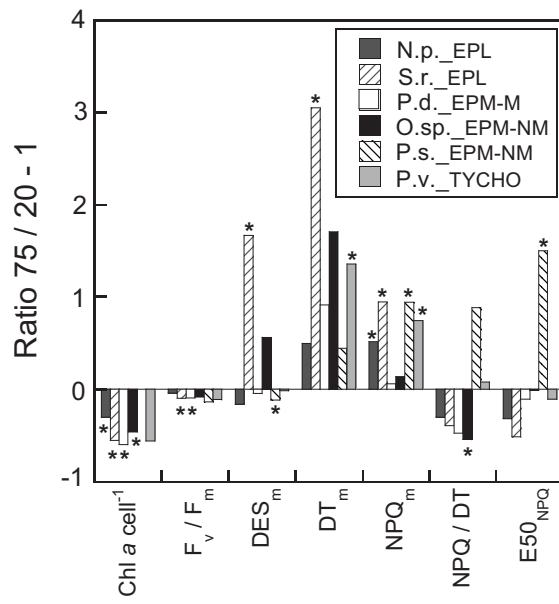
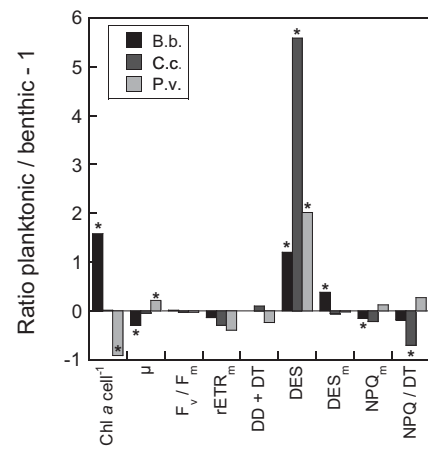


Figure 5



Species	Growth form		Collection n°	Sampling place	Average biovolume (µm ³)
<i>Craspedostauros britannicus</i> C.b.	Epipelon (EPL)		NCC195-06-2	Pouliguen, Atlantic, France	1740
<i>Entomoneis paludosa</i> E.p.			NCC18-1	Bay of Bourgneuf, Atlantic, France	1081
<i>Halamphora coffeaeformis</i> H.c.			UTCC58	Victoria, British Columbia, Pacific, Canada	126
<i>Navicula phyllepta</i> N.p.			CCY9804	Westerschelde estuary, North sea, The Netherlands	218
<i>Seminavis robusta</i> S.r.			DCG 0105	Progeny of strains from Veerse Meer, The Netherlands	1790
<i>Amphora</i> sp. A. sp.	Epipsammon (EPM)	motile (EPM-M)	DCG 0493	Rammekenshoek, North sea, The Netherlands	39
<i>Nitzschia</i> cf. <i>frustulum</i> N.f.			DCG 0494	Rammekenshoek, North Sea, The Netherlands	29
<i>Planothidium delicatulum</i> P.d.			NCC363	Bay of Bourgneuf, Atlantic, France	242
<i>Biremis lucens</i> B.l.		non-motile (EPM-NM)	NCC360.2	Bay of Bourgneuf, Atlantic, France	242
<i>Fragilaria</i> cf. <i>subsalina</i> F.s.			DCG 0492	Rammekenshoek, North sea, The Netherlands	165
<i>Opephora</i> sp. O. sp.			DCG 0448	Rammekenshoek, North Sea, The Netherlands	86
<i>Plagiogramma staurophorum</i> P. s.			DCG 0495	Rammekenshoek, North sea, The Netherlands	n.d.
<i>Brockmanniella brockmannii</i> B.b.	Tychoplankton (TYCHO)		NCC161	Bay of Bourgneuf, Atlantic, France	105
<i>Cylindrotheca closterium</i> C.c.			Collection Univ. Aveiro	Ria de Aveiro, Atlantic, Portugal	247
<i>Plagiogrammopsis vanheurckii</i> P.v.			NCC186-2	Bay of Bourgneuf, Atlantic, France	737

Table 2

Parameter	Unit	Definition	Photophysiological meaning	Measurement conditions
F_0	No units	Minimum PSII Chl fluorescence yield	Used to calculate F_v/F_m (see below)	Measured with NSLCs after 15 min of dark acclimation
F_m	No units	Maximum PSII Chl fluorescence yield	Used to calculate F_v/F_m and NPQ (see below)	Measured with NSLCs during a saturating pulse after 15 min of dark acclimation
F_v/F_m	No units	Maximum photosynthetic efficiency of PSII; $F_v = F_m - F_0$	Maximum quantum efficiency of PSII photochemistry	See the above measurement conditions for F_0 and F_m
F_m'	No units	F_m for illuminated cells	Used to measure NPQ and rETR	Measured with NSLCs during a saturating pulse after 5 min of illumination at specific E
NPQ	No units	Non-photochemical quenching of Chl fluorescence; $NPQ = F_m'/F_m' - 1$	Estimates the photoprotective dissipation of excess energy	Measured with NSLCs
rETR	$\mu\text{mol electrons m}^{-2} \text{s}^{-1}$	Relative electron transport rate of PSII; $rETR = \Phi_{PSII} \times E$ where $\Phi_{PSII} = F_m' - F/F_m'$	Effective quantum yield of photochemistry vs. E	Measured with RLCs; F is the steady-state of Chl fluorescence measured after 30 s illumination at a given E
α	Relative units	rETR-E curve initial slope	Maximum light efficiency use	Derived from fitted rETR-E curves measured with RLCs (Eilers and Peeters, 1988)
$rETR_m$	$\mu\text{mol electrons m}^{-2} \text{s}^{-1}$	rETR-E curve asymptote	Maximum relative photosynthetic electron transport rate	Derived from fitted rETR-E curves measured with RLCs (Eilers and Peeters, 1988)
E_k	$\mu\text{mol photons. m}^{-2} \text{s}^{-1}$	$E_k = rETR_m / \alpha$	Light saturation coefficient	Derived from fitted rETR-E curves measured with RLCs (Eilers and Peeters, 1988)
NPQ_m	No units	NPQ-E curve asymptote	Maximum NPQ	Measured with NSLCs
$E50_{NPQ}$	$\mu\text{mol photons. m}^{-2} \text{s}^{-1}$	E for reaching 50% of NPQ_m	Pattern of NPQ induction vs. E	Derived from fitted NPQ-E curves (Seródio and Lavaud, 2011) measured with NSLCs
n_{NPQ}	No units	NPQ-E curve sigmoidicity coefficient	Onset of NPQ induction for moderate E_s ($< E50_{NPQ}$)	Derived from fitted NPQ-E curves (Seródio and Lavaud, 2011) measured with NSLCs
DT_m	$\text{mol. } 100 \text{ mol Chl } \alpha^{-1}$	DT-E curve asymptote	Maximum DT concentration	Measured with NSLCs
$E50_{DT}$	$\mu\text{mol photons. m}^{-2} \text{s}^{-1}$	E for reaching 50% of DT_{max}	Pattern of DT synthesis vs. E	Derived from fitted DT-E curves (Seródio and Lavaud, 2011) measured with NSLCs
n_{DT}	No units	DT-E curve sigmoidicity coefficient	Onset of DT synthesis for moderate E_s ($< E50_{NPQ}$)	Derived from fitted DT-E curves (Seródio and Lavaud, 2011) measured with NSLCs
DES_m	%	DES-E curve asymptote; $DES = [DT / (DD+DT) \times 100]$	Maximum de-epoxidation state	Measured with NSLCs
NPQ / DT	No units	NPQ-DT curve slope	Effective involvement of DT in NPQ for all E_s (Lavaud et Lepetit, 2013)	Measured with NSLCs

Table 3

Growth Form	Pigments							Photosynthetic parameters				
	μ	Chl <i>a</i> cell ⁻¹	Chl <i>c</i>	Fx	β -car	DD+DT	DES	F _v /F _m	α	rETR _m	E _k	PSII CET _m
EPL	1.66 ± 0.12	12.55 ± 12.91	18.91 ± 3.05	65.99 ± 7.90	3.91 ± 0.39	6.39 ± 0.61	0.75 ± 0.93	0.72 ± 0.01	0.68 ± 0.03	52.41 ± 5.90	78.93 ± 9.79	2.09 ± 0.23
EPM-M	1.56 ± 0.14	1.45 ± 0.78	16.05 ± 3.34	64.29 ± 10.21	2.76 ± 0.43	10.34 ± 1.17	4.25 ± 1.79	0.68 ± 0.02	0.65 ± 0.04	51.50 ± 7.36	80.41 ± 12.89	2.86 ± 0.33
EPM-NM	1.45 ± 0.12	2.13 ± 1.63	20.12 ± 3.63	70.52 ± 8.83	2.11 ± 0.43	11.52 ± 1.13	2.30 ± 1.33	0.67 ± 0.02	0.63 ± 0.04	39.20 ± 4.88	61.01 ± 8.52	2.82 ± 0.23
TYCHO	1.61 ± 0.14	1.72 ± 2.45	24.81 ± 5.17	79.36 ± 10.12	3.04 ± 0.51	9.25 ± 1.09	4.29 ± 1.83	0.73 ± 0.02	0.71 ± 0.04	58.32 ± 8.44	82.79 ± 13.40	2.03 ± 0.26

Table 4

Growth form	NPQ _m	E50 _{NPQ}	n _{NPQ}	DES _m	DT _m	E50 _{DT}	n _{DT}	NPQ/DT
EPL	0.69 ± 0.09	866.45 ± 200.24	1.88 ± 0.26	21.20 ± 3.38	1.34 ± 0.52	714.73 ± 128.29	2.39 ± 0.20	0.46 ± 0.10
EPM-M	1.71 ± 0.28	1061.25 ± 310.20	2.04 ± 0.34	28.68 ± 4.37	3.08 ± 1.36	809.41 ± 164.71	1.38 ± 0.20	0.52 ± 0.14
EPM-NM	2.41 ± 0.34	360.61 ± 91.42	2.27 ± 0.29	29.43 ± 3.79	3.45 ± 2.21	465.91 ± 80.04	2.30 ± 0.21	0.67 ± 0.16
TYCHO	0.66 ± 0.11	3887.42 1105.58	1.12 ± 0.34	22.73 ± 4.39	1.78 ± 0.61	1099.82 ± 341.05	1.42 ± 0.19	0.36 ± 0.10